APPLIED AND ENVIRONMENTAL MICROBIOLOGY, May 2006, p. 3321–3329 Vol. 72, No. 5
0099-2240/06/$08.00+0 doi:10.1128/AEM.72.5.3321–3329.2006

Characterization of Novel Carbazole Catabolism Genes from Gram-Positive Carbazole Degrader *Nocardioides aromaticivorans* IC177†

Kengo Inoue, Hiroshi Habe, Hisakazu Yamane, and Hideaki Nojiri*

Biotechnology Research Center, The University of Tokyo, 1-1-1 Yayoi, Bunkyo-ku, Tokyo 113-8657, Japan

Received 21 December 2005/Accepted 28 February 2006

Nocardioides aromaticivorans **IC177 is a gram-positive carbazole degrader. The genes encoding carbazole degradation (*car* genes) were cloned into a cosmid clone and sequenced partially to reveal 19 open reading frames. The *car* genes were clustered into the *carAaCBaBbAcAd* and *carDFE* gene clusters, encoding the enzymes responsible for the degradation of carbazole to anthranilate and 2-hydroxypenta-2,4-dienoate and of 2-hydroxypenta-2,4-dienoate to pyruvic acid and acetyl coenzyme A, respectively. The conserved amino acid motifs proposed to bind the Rieske-type [2Fe-2S] cluster and mononuclear iron, the Rieske-type [2Fe-2S] cluster, and flavin adenine dinucleotide were found in the deduced amino acid sequences of *carAa*, *carAc*, and *carAd*, respectively, which showed similarities with CarAa from *Sphingomonas* sp. strain KA1 (49% identity), CarAc from *Pseudomonas resinovorans* CA10 (31% identity), and AhdA4 from *Sphingomonas* sp. strain P2 (37% identity), respectively. *Escherichia coli* cells expressing CarAaAcAd exhibited major carbazole 1,9a-dioxygenase (CARDO) activity. These data showed that the IC177 CARDO is classified into class IIB, while gram-negative CARDOs are classified into class III or IIA, indicating that the respective CARDOs have diverse types of electron transfer components and high similarities of the terminal oxygenase. Reverse transcription-PCR (RT-PCR) experiments showed that the *carAaCBaBbAcAd* and *carDFE* gene clusters are operonic. The results of quantitative RT-PCR experiments indicated that transcription of both operons is induced by carbazole or its metabolite, whereas anthranilate is not an inducer. Biotransformation analysis showed that the IC177 CARDO exhibits significant activities for naphthalene, carbazole, and dibenzo-*p*-dioxin but less activity for dibenzofuran and biphenyl.**

Carbazole is an *N*-heterocyclic aromatic compound derived from creosote, crude oil, and shale oil (32, 33). Carbazole is known to be both mutagenic and toxic (1) but has been used as an industrial raw material for the production of dyes, medicines, and plastics (3). Various carbazole-degrading bacteria have been reported in studies examining the mechanisms of biodegradation of this recalcitrant compound and the application of bacteria in bioremediation (39). The carbazole biodegradation pathway of *Pseudomonas resinovorans* CA10 has been elucidated (41), and carbazole catabolic genes (*car* genes) from this organism have been studied extensively. In CA10, the carbazole 1,9a-dioxygenase (CARDO; encoded by *carAa*, *carAc*, and *carAd*), the *meta*-cleavage enzyme (encoded by *carBa* and *carBb*), and the *meta*-cleavage compound hydrolase (encoded by *carC*) together are involved in the conversion of carbazole to anthranilate and 2-hydroxypenta-2,4-dienoate (Fig. 1) (47, 48). 2-Hydroxypenta-2,4-dienoate is converted to pyruvic acid and acetyl coenzyme A by 2-hydroxypenta-2,4-dienoate hydratase (encoded by *carD*), 4-hydroxy-2-oxovalerate aldolase (encoded by *carE*), and acetaldehyde dehydrogenase (encoded by *carF*) (Fig. 1) (40). Dihydroxylation by the initial oxygenase is often a critical step for aerobic bacterial degradation of aromatic compounds. The Rieske nonheme iron oxygenase systems (ROSs) catalyzing dihydroxylation typically consist of two or three components that comprise an electron transfer chain mobilizing electrons from NADH or NADPH, via flavin and [2Fe-2S] redox centers, to the site of dioxygen activation (5, 11, 29). The ROSs have historically been classified into five groups (IA, IB, IIA, IIB, and III) based on their numbers of constituents and the nature of their redox centers (2). The three-component systems consisting of terminal oxygenase, ferredoxin, and ferredoxin reductase have been classified into groups IIA, IIB, and III. In groups IIA and IIB, ROSs have putidaredoxin homologs and the Rieske-type ferredoxin, respectively, as the ferredoxin component but commonly have a ferredoxin reductase component that contains flavin adenine dinucleotide (FAD). The class III ROSs have the Rieske-type ferredoxin and a reductase which contains FAD and a chloroplast-type [2Fe-2S] cluster. The CARDO from CA10 is classified as a class III ROS according to the above classification (35, 47). *Sphingomonas* sp. strain KA1 possesses the *carAaIBaIBbICIAcI* genes, which are located on the 254-kb circular plasmid pCAR3 (16, 19, 56). As a result of the determination of the complete nucleotide sequence of pCAR3, a second copy of the *car* gene cluster (*carAaIIBaIIBbIICIIAcII*), a ferredoxin gene (*fdxI*), and two ferredoxin reductase genes (*fdrII* and *fdrII*) were identified (56). In the CARDO of KA1, putidaredoxin-type ferredoxins (CarAcI, CarAcII, and FdxI) mediate electron transport from ferredoxin reductases (FdrI and FdrII) to the terminal oxygenases (CarAaI and CarAaII), suggesting that the CARDO from KA1 is affiliated with a class IIA oxygenase.

Carbazole degradation by gram-negative bacteria has been studied genetically in detail. However, there are no reports about carbazole catabolic genes from gram-positive bacteria. Some gram-positive bacteria, such as actinomycetes, can min-

* Corresponding author. Mailing address: Biotechnology Research Center, The University of Tokyo, 1-1-1 Yayoi, Bunkyo-ku, Tokyo 113-8657, Japan. Phone: 81-3-5841-3064. Fax: 81-3-5841-8030. E-mail: anojiri@mail.ecc.u-tokyo.ac.jp.

† Supplemental material for this article may be found at http://aem.asm.org/.

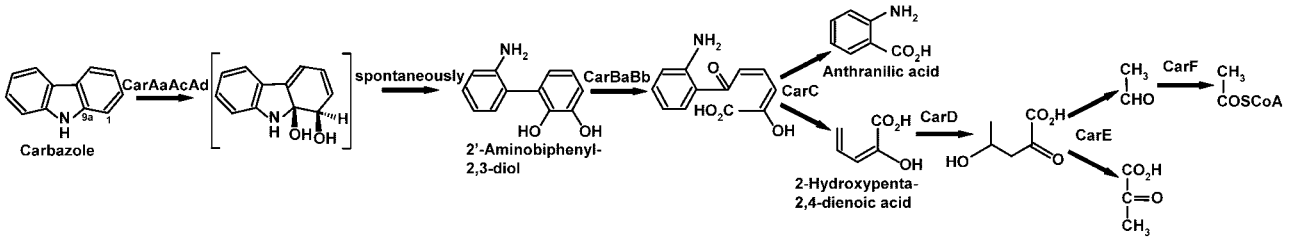

FIG. 1. Pathway for degradation of carbazole by gram-negative *P. resinovorans* CA10 (40, 41) and gram-positive *N. aromaticivorans* IC177.

eralize various recalcitrant molecules (30). *Nocardioides* species, which belong to the *Actinomycetales*, have been shown to degrade a variety of aromatic compounds, including 2,4,6-trinitrophenol, 2,4,5-trichlorophenoxyacetic acid, *p*-nitrophenol, phenanthrene, and dibenzofuran (9, 13, 15, 20, 25, 45). Recently, we isolated a carbazole degrader, *Nocardioides aromaticivorans* (formally *Nocardioides* sp.) IC177 (18). IC177 accumulates anthranilate in culture during biodegradation of carbazole as well as the gram-negative carbazole degrader CA10 (18, 41). This strain can also grow on protocatechuate, dibenzothiophene sulfone, and anthranilate as the sole source of carbon (18). Degenerate PCR experiments using primers for amplifying the internal fragment of the *carAa* gene revealed that IC177 possesses *carAa* and *carC* homologs (18).

For this study, we characterized the genes for carbazole degradation and determined the catabolic pathway of carbazole to anthranilate in a gram-positive bacterium. We also demonstrated the operonic structure of the *car* gene clusters and their inducibility by reverse transcription-PCR (RT-PCR) and quantitative RT-PCR (qRT-PCR). The substrate preference of the initial carbazole oxygenase from IC177 was also investigated.

MATERIALS AND METHODS

Bacterial strains, plasmids, and culture conditions. The bacterial strains, plasmids, and cosmids used in this study are listed in Table 1. The medium used for bacterial growth was Luria-Bertani (LB) medium (46). *Escherichia coli* JM109 (46) and DH5α (46) were used as host strains for the plasmids pBluescript II SK(−), SuperCos1, and their derivatives. Ampicillin (50 μg/ml), kanamycin (50 μg/ml), and chloramphenicol (30 μg/ml) were added to selective media. For plate cultures, the above-described media solidified with 1.6% (wt/vol) agar were used.

DNA manipulations. DNA techniques were performed according to standard methods (46). Total DNA of IC177 grown on LB medium at 30°C and plasmid and cosmid DNAs from *E. coli* host cells were prepared as described previously (40). DNA fragments were extracted from agarose gels by using a QIAEX II DNA extraction kit (QIAGEN, Hilden, Germany) according to the manufacturer's instructions.

Cloning of DNA containing the *car* genes. We constructed a genomic cosmid library of IC177 as described previously (40), except that we used the restriction endonuclease Sau3AI instead of EcoRI to prepare the vector arm of SuperCos1 and partially digested genomic DNA. To screen the positive cosmid clones containing the *car* gene clusters of IC177, we conducted colony hybridization using probes prepared from the 991-bp DNA fragment containing partial *carAa* and *carC* from IC177 (insert of pT177001) (Table 1), as previously described (40). Southern hybridization analysis of endonuclease-digested DNA of IC177 was performed under stringent conditions according to previously described methods (40). A positive cosmid clone designated pCS1770033 was used for further analyses.

Nucleotide sequence determination, homology searches, and alignment analysis. Nucleotide sequences were determined using the GPS-1 genome priming system (New England Biolabs, Ipswich, MA) as described previously (40). The nucleotide sequences obtained were analyzed with DNASIS-Mac software (version 3.7; Hitachi Software Engineering, Yokohama, Japan). Nucleotide and deduced amino acid sequences were searched for similarities by using the BLAST program (http:/www.ncbi.nlm.nih.gov/BLAST/). Amino acid sequence alignment analysis and phylogenetic analysis were performed by using the ClustalW program at the DDBJ website (http://www.ddbj.nig.ac.jp). Phylogenetic trees were produced with the TreeView program (42).

RNA extraction and RT-PCR. Cells for RNA extraction were harvested from 5 ml NMM2 culture containing carbazole (0.1% [wt/vol]) after 5 days of incubation. NMM2 had the following composition: Na_2HPO_4, 2.2 g/liter; KH_2PO_4, 0.8 g/liter; $MgSO_4 \cdot 7H_2O$, 0.2 g/liter; NH_4NO_3, 3 g/liter; $FeSO_4 \cdot 7H_2O$, 0.01 g/liter; and $CaCl_2 \cdot 2H_2O$, 0.01 g/liter. Harvested cells were resuspended in 100 μl distilled water containing 2 mg/ml lysozyme and incubated at 37°C for 1 h. Total RNA was prepared with Sepasol-RNA I Super (Nacalai Tesque, Kyoto, Japan) according to the manufacturer's instructions. Contaminating DNA in total RNA preparations was removed with RQ1 RNase-free DNase (Promega, Madison, WI). RT-PCR was performed in 25-μl reaction mixtures containing 200 ng total RNA and 10 pmol of each primer with a OneStep RNA PCR kit (Takara, Tokyo, Japan). The thermocycler program used for RT-PCR was as follows: 60°C for 30 min; 94°C for 2 min; 30 cycles of 96°C for 30 s, 55°C for 30 s, and 72°C for 2 min; and 72°C for 7 min. The nucleotide sequences of the eight primer sets used for RT-PCR are shown in Table S1 in the supplemental material.

qRT-PCR. After cultivation in 5 ml of NMM2 containing succinate (0.1% [wt/vol]) at 30°C for 4 days, succinate (0.1% [wt/vol]), succinate (0.08% [wt/vol]) plus anthranilate (0.02% [wt/vol]), or succinate (0.08% [wt/vol]) plus carbazole (0.02% [wt/vol]) was added to the resultant IC177 cultures. The concentration of all added stock solutions was 10% (wt/vol). After incubation of each culture at 30°C for 1, 4, and 8 h, total RNA was isolated as described above. qRT-PCR was performed using Quantitect SYBR green RT-PCR (QIAGEN) on an ABI PRISM 7700 sequence detection system (Applied Biosystems, Foster City, CA). The total volume of the reaction mixture was 20 μl and contained 80 ng (or 8 pg for *rrn* gene detection) RNA. The primer sets used for amplification of partial *carAa*, *carD*, and *rrn* genes in qRT-PCR analysis are shown in Table S1 in the supplemental material. The thermal cycling conditions were as follows: 30 min at 55°C, 15 min at 95°C, and 40 cycles of 30 s at 96°C, 30 s at 55°C, and 30 s at 72°C. A negative control (distilled water instead of the RNA solution) and an RNA sample without the reverse transcription step (to determine genomic DNA contamination) were included. For each measurement, a standard curve was generated by using appropriately diluted target DNA fragments. Relative quantification was based on the levels of *carD* and *carAa* mRNAs compared to that of *rrn* as a reference gene. For each RNA extraction, measurements of gene expression were obtained in triplicate.

Construction of expression plasmids. To express the *car* genes under control of the *lac* promoter in *E. coli*, we constructed pB177301 (for the expression of *carAa*), pB177302 (*carAc*), pB177304 (*carAaAc*), pB177305 (*carAaAd*), pB177306 (*carAcAd*), pB177307 (*carAaAcAd*), pB177308 (*carAaAcAdBa*), pB177309 (*carAaAcAdBaBb*), and pB177310 (*carAaAcAdBaBbC*) (Table 1). Each *car* gene, including an artificial Shine-Dalgarno (SD) sequence (51), was amplified by PCR from pSC1770033 and its derivatives, using the primers shown in the supplemental material. Each PCR product containing *carAa*, *carAc*, *carAd*, *carBa*, *carBb*, or *carC* was ligated into the pT7Blue T-vector (Novagen, Madison, WI), and the resultant plasmids were designated pT177201, pT177202, pT177203, pT177204, pT177205, and pT177206, respectively. The nucleotide sequence of each insert was checked with the original sequence. All of the inserts of the plasmids possessed an XbaI site and an SD sequence upstream of each *car* gene, with a SpeI site immediately downstream of the termination codon for each *car* gene. pT177201 was digested with XbaI and SpeI. A 1.2-kb XbaI-SpeI fragment containing the SD sequence and the *carAa* gene was gel purified. The

TABLE 1. Bacterial strains, plasmids, and cosmids used in this study

Strain, plasmid, or cosmid	Relevant characteristics	Source or reference
Bacterial strains		
Escherichia coli JM109	*recA1 supE44 endA1 hsdR17* Δ(*lac-proAB*) *gyrA96 relA1 thi* [F′ *traD36 proAB*$^+$ *lacI*^{q}*ZΔM15*]	46
Escherichia coli DH5α	*supE44* Δ*lacU169* ϕ*80dlacZΔM15 hsdR17 recA1 endA1 gyrA96 thi-1 relA1*	46
Nocardioides aromaticivorans IC177	Car^{+a}	18
Plasmids		
pBluescript II SK(−)	Ap^r *lacZ*, pMB9 replicon	Stratagene
pB177101	Ap^r, pBluescript II SK(−) with 12.2-kb NotI insert of IC177 DNA	This study
pB177102	Ap^r, pBluescript II SK(−) with 6.5-kb NotI-EcoRV insert of IC177 DNA	This study
pB177103	Ap^r, pBluescript II SK(−) with 3.0-kb XhoI insert of IC177 DNA	This study
pB177104	Ap^r, pBluescript II SK(−) with 5.5-kb EcoRV-NotI insert of IC177 DNA	This study
pB177105	Ap^r, pBluescript II SK(−) with 2.5-kb SacI insert of IC177 DNA	This study
pB177106	Ap^r, pBluescript II SK(−) with 3.7-kb BamHI insert of IC177 DNA	This study
pB177107	Ap^r, pBluescript II SK(−) with 1.2-kb BamHI insert of IC177 DNA	This study
pB177301	Ap^r, pBluescript II SK(−) with 1.2-kb insert containing *carAa* gene of IC177	This study
pB177302	Ap^r, pBluescript II SK(−) with 0.3-kb insert containing *carAc* gene of IC177	This study
pB177304	Ap^r, pBluescript II SK(−) with 1.6-kb insert containing *carAaAc* genes of IC177	This study
pB177305	Ap^r, pBluescript II SK(−) with 2.4-kb insert containing *carAaAd* genes of IC177	This study
pB177306	Ap^r, pBluescript II SK(−) with 1.6-kb insert containing *carAcAd* genes of IC177	This study
pB177307	Ap^r, pBluescript II SK(−) with 2.8-kb insert containing *carAaAcAd* genes of IC177	This study
pB177308	Ap^r, pBluescript II SK(−) with 3.1-kb insert containing *carAaAcAdBa* genes of IC177	This study
pB177309	Ap^r, pBluescript II SK(−) with 3.9-kb insert containing *carAaAcAdBaBb* genes of IC177	This study
pB177310	Ap^r, pBluescript II SK(−) with 4.8-kb insert containing *carAaAcAdBaBbC* genes of IC177	This study
pT177001	Ap^r, pT7Blue(R) with 991-bp degenerate PCR-amplified DNA fragment containing partial *carAaC* genes of IC177	18
pT177201	Ap^r, pT7Blue(R) with 1.2-kb PCR-amplified DNA fragment containing *carAa* gene of IC177	This study
pT177202	Ap^r, pT7Blue(R) with 0.4-kb PCR-amplified DNA fragment containing *carAc* gene of IC177	This study
pT177203	Ap^r, pT7Blue(R) with 1.2-kb PCR-amplified DNA fragment containing *carAd* gene of IC177	This study
pT177204	Ap^r, pT7Blue(R) with 0.3-kb PCR-amplified DNA fragment containing *carBa* gene of IC177	This study
pT177205	Ap^r, pT7Blue(R) with 0.8-kb PCR-amplified DNA fragment containing *carBb* gene of IC177	This study
pT177206	Ap^r, pT7Blue(R) with 0.9-kb PCR-amplified DNA fragment containing *carC* gene of IC177	This study
pT7Blue(R)	Ap^r *lacZ*	Novagen
pUCARA	Ap^r, pUC119 with 5.6-kb EcoRI insert of CA10 DNA	47
SuperCos1	Ap^r Km^r cos	Stratagene
Cosmid		
pSC1770033	Ap^r, SuperCos1 with Sau3AI insert of IC177 DNA containing *car* gene cluster	This study

[a] Car$^+$ indicates an ability to grow on carbazole as the sole source of carbon, nitrogen, and energy.

1.2-kb XbaI-SpeI fragment was ligated into the SpeI site of pBluescript II SK(−) to give pB177301, taking advantage of the identical nucleotide sequences at the staggered end of the SpeI site and that of XbaI. The resultant plasmid was digested with the appropriate enzymes to check the orientation of the insert. The *carAa* gene in pB177301 was under the control of the *lac* promoter and an SD sequence. The 0.4-kb XbaI-SpeI fragment containing the SD sequence and the *carAc* gene was prepared from pT177202 and ligated into the SpeI site of pB177301 (*carAa*) to give pB177304 (*carAaAc*). The pB177302 (*carAc*), pB177305 (*carAaAc*), pB177306 (*carAcAd*), pB177307 (*carAaAcAd*), pB177308 (*carAaAcAdBa*), pB177309 (*carAaAcAdBaBb*), and pB177310 (*carAaAcAdB aBbC*) plasmids were constructed in a similar manner.

Biotransformation analysis. *Escherichia coli* JM109 cells carrying plasmid pBluescript II SK(−) (negative control), pB177301, pB177304, pB177305, pB177306, pB177307, pB177310, or pUCARA (positive control) (47) were cultured for 8 h at 37°C in 5 ml LB medium containing ampicillin (50 μg/ml). The culture was transferred to 250 ml fresh LB medium and further cultured at 37°C. After 2 h of incubation, isopropyl-β-D-thiogalactopyranoside (IPTG) was added to a final concentration of 1 mM to induce gene expression, and the cells were harvested after 8 h by centrifugation. The collected cells were washed twice with CNF buffer and resuspended in the buffer at an optical density at 600 nm of 20 to 30. CNF buffer had the following composition: Na_2HPO_4, 2.2 g/liter; and KH_2PO_4, 0.8 g/liter. A reaction mixture consisting of 3 ml cell suspension and 0.01% (wt/vol) (0.46 to 0.78 mM) substrate was placed in a test tube and shaken at 285 strokes per min at 37°C. After 24 h of incubation, the mixture was extracted with an equal volume of ethyl acetate. For detection of anthranilate formed from carbazole, the incubated culture was acidified to pH 3 with 1 N HCl prior to the ethyl acetate extraction. The ethyl acetate layer was dried over anhydrous sodium sulfate. A portion of each extract was analyzed using a JMS-Automass 150 gas chromatography-mass spectrometry (GC-MS) system (JEOL, Tokyo, Japan) as previously described (18). The substrates and products were identified by comparison with previously analyzed retention times and MS spectra (18, 21, 38, 53).

Nucleotide sequence accession numbers. The nucleotide sequences reported in this study have been deposited in the DDBJ, EMBL, and GenBank nucleotide sequence databases. The nucleotide sequence data for the 17,582-bp NotI-BamHI fragment of IC177 was registered under accession no. AB244528.

RESULTS

Cloning and sequencing of *car* genes from IC177. The nucleotide sequence of the 16S rRNA gene from IC177 is most similar to that of *N. aromaticivorans* H-1^T (99.6% identity), as recently described (25). Due to this similarity, we concluded that IC177 belongs to this species, and we renamed it accordingly.

A 991-bp DNA fragment containing tandemly linked partial *carAa* and *carC* homologs was previously obtained by PCR experiments using degenerate primers for *carAa* (18). A cosmid clone containing the above-described 991-bp region was

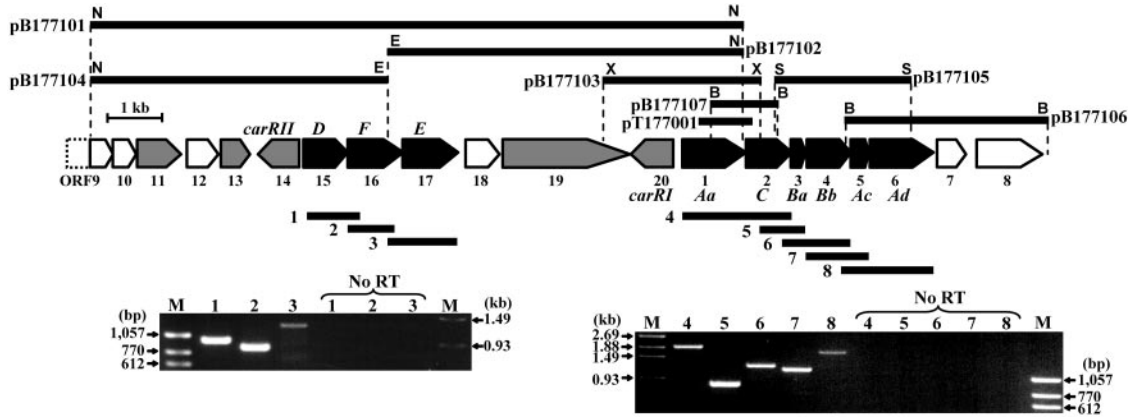

FIG. 2. Genetic organization of *car* gene clusters and their flanking regions in *N. aromaticivorans* IC177 and electrophoresis of RT-PCR products. The pentagons indicate the sizes, locations, and directions of ORF transcription. The *car* genes are shown by black pentagons. Gray pentagons indicate the putative transcriptional regulators. Black bars indicate the locations of the subcloned DNA fragments or locations of the expected RT-PCR products for each lane. Restriction sites are indicated as follows: B, BamHI; E, EcoRV; S, SacI; N, NotI; and X, XhoI. Only restriction sites relevant to the clones and constructs described in this figure are shown.

selected from an IC177 cosmid library by colony hybridization and designated pSC1770033. The nucleotide sequence of a 17,582-bp (NotI-BamHI) region in pSC1770033 containing the *carAa* and *carC* gene homologs was determined. The positions and lengths of the inserts of the subclones used for sequencing analysis are shown in Fig. 2. The G+C content of the 17,582-bp region was uniformly high (67.3%). The 17,582-bp region contained 19 complete open reading frames (ORFs) and a partial ORF (ORF9). Similarities between the ORFs and representative homologs are summarized in Table 2.

The amino acid sequence of ORF1 showed similarity to CarAa, the terminal oxygenase component of carbazole 1,9a-

TABLE 2. Proposed functions of proteins encoded by ORFs identified in a 17,582-bp region of the IC177 genome

ORF (gene)	Position[a]	Probable function	Homology			
			Amino acid identity (%)[b]	Name of protein	Source	Accession no.
ORF9	1–432	Oxidoreductase	59	Putative oxidoreductase	*Streptomyces coelicolor* A3(2)	CAC44594
ORF10	429–866	Thioesterase	26	Probable 4-hydroxybenzoyl-CoA thioesterase	*Pirellula* sp. strain 1	CAD78650
ORF11	872–1,672	Transcriptional regulator	37	Putative regulator	*Streptomyces avermitilis* MA-4680	BAC70019
ORF12	1,780–2,358	Unknown		Hypothetical protein		
ORF13	2,403–2,948	Transcriptional regulator	23	TetR family transcriptional regulatory protein	*Gloeobacter violaceus* PCC 7421	BAC88612
ORF 14 (*carRII*)	3,085–3,849	Transcriptional regulator	36	CarRI	*N. aromaticivorans* IC177	This study
ORF15 (*carD*)	3,919–4,734	2-Hydroxypenta-2,4-dienoate hydratase	49	Putative 2-keto-4-pentenoate hydratase	*Pseudomonas putida* strain RR21	CAE92879
ORF16 (*carF*)	4,731–5741	Acetaldehyde dehydrogenase (acylating)	64	Acetaldehyde dehydrogenase	*Azotobacter vinelandii*	ZP_00092919
ORF17 (*carE*)	5,738–6,760	4-Hydroxy-2-oxovalerate aldolase	67	XylK	*N. aromaticivorans* F199	AAD03993
ORF18	6,881–7,501	Unknown				
ORF19	7,568–9,910	Transcriptional regulator	36	Putative regulator	*S. coelicolor* A3(2)	CAB93384
ORF20 (*carRI*)	9,917–10,705	Transcriptional regulator	36	CarRII	*N. aromaticivorans* IC177	This study
ORF1 (*carAa*)	10,860–12,026	Terminal oxygenase component of carbazole 1,9a-dioxygenase	49	CarAa	*Sphingomonas* sp. strain KA1	BAC56759
ORF2 (*carC*)	12,023–12,862	*meta*-Cleavage compound hydrolase	45	CarC	*Sphingomonas* sp. strain KA1	BAC56762
ORF3 (*carBa*)	12,859–13,134	Subunit of *meta*-cleavage enzyme	29	CarBa	*Janthinobacterium* sp. strain J3	BAC56743
ORF4 (*carBb*)	13,134–13,949	Subunit of *meta*-cleavage enzyme	39	CarBb	*Sphingomonas* sp. strain KA1	BAC56761
ORF5 (*carAc*)	13,949–14,296	Ferredoxin component of carbazole 1,9a-dioxygenase	36	Putative dioxygenase ferredoxin subunit	*S. avermitilis* MA-4680	BAC74038
ORF6 (*carAd*)	14,296–15,468	Ferredoxin reductase component of carbazole 1,9a-dioxygenase	38	Ferredoxin reductase	*Mycobacterium tuberculosis*	AAK44942
ORF7	15,528–16,058	Unknown				
ORF8	16,253–17,461	Transposase	34	Putative transposase	*S. avermitilis* MA-4680	BAC68012

[a] Positions in 17,582-bp DNA region sequenced in this study (accession no. AB244528).
[b] Values were calculated only for the sequenced region.

dioxygenase, from KA1 and CA10 (49 and 45% identity, respectively). The consensus sequences of Rieske-type iron-sulfur proteins for the binding of a [2Fe-2S] cluster and mononuclear nonheme iron (36, 43) were determined. The amino acid sequences of ORF2, ORF3, and ORF4 from IC177 showed similarities to the *meta*-cleavage compound hydrolase CarC (45% identity), the 2′-aminobiphenyl-2,3-diol 1,2-dioxygenase small subunit CarBa (19% identity), and the large subunit CarBb (39% identity), respectively, from KA1. The deduced amino acid sequence of ORF5 contained a conserved sequence for Rieske-type [2Fe-2S] clusters and showed similarity to CarAc from CA10 (31% identity) (34) and the ferredoxin component of biphenyl dioxygenase BphF from *Acidovorax* sp. strain KKS102 (20% identity) (10). The deduced amino acid sequence of ORF6 possessed FAD-binding and NADH-binding domains (29, 49) and showed major similarity to the ferredoxin reductase components of initial oxygenases of aromatic compounds, such as AhdA4 (ferredoxin reductase component of salicylate dioxygenase) from *Sphingomonas* sp. strain P2 (37% identity) (44) and BphA4 (ferredoxin reductase component of biphenyl dioxygenase) from *Acidovorax* sp. strain KKS102 (28%) (22). Thus, following the nomenclature of CA10, these six ORFs were designated *carAa*, *carC*, *carBa*, *carBb*, *carAc*, and *carAd* (Fig. 2).

In a region 4.1 to 6.9 kb upstream of the initiation codon of the *carAa* gene, ORF15, ORF16, and ORF17 were identified (Fig. 2). The deduced amino acid sequences of ORF15, ORF16, and ORF17 showed similarities to 2-hydroxypenta-2,4-dienoate hydratase, acetaldehyde dehydrogenase (acylating), and 4-hydroxy-2-oxovalerate aldolase, respectively, whose genes have been identified in various aromatic-compound-degrading bacteria, such as *bphEGF* in *Acidovorax* sp. strain KKS102 (23) and *Rhodococcus* sp. strain RHA1 (28), *todGIH* in *P. putida* F1 (26), *dmpEFG* in *Pseudomonas* sp. strain CF600 (52), and *carDFE* in *P. resinovorans* CA10 (40). Putative crucial residues for dehydrogenase activity and putative metal iron ligands were identified on the basis of the crystal structures of DmpF and DmpG, which functionally correspond to CarF and CarE, respectively (27). The *carDFE* gene products were thought to function as *meta*-pathway enzymes for carbazole catabolism in IC177 (Fig. 1 and 2).

The deduced amino acid sequence of ORF20, located immediately upstream of the *carAaCBaBbAcAd* gene cluster, showed high homology with transcriptional regulators classified in the IclR family. The putative regulatory gene (tentatively designated *carRI*) was transcribed in the opposite direction from that of the *carAaCBaBbAcAd* genes (Fig. 2), implying that this gene product functions as a transcriptional regulator of the *carAaCBaBbAcAd* genes. Members of the IclR family of regulatory proteins are generally transcriptional repressors, but those that control catabolic pathways have all been described as activators (54). Moreover, a putative transcriptional regulatory gene (designated *carRII*) located immediately upstream of the *carD* gene was identified (Fig. 2). The deduced amino acid sequence of CarRII also showed similarity to the transcriptional regulators in the IclR family, with the greatest similarity to CarRI (36% identity) (Table 2).

Operonic structures and *car* gene inducibility. To confirm that the identified *car* genes are actually expressed as a single transcriptional unit in response to carbazole exposure, RT-PCR experiments were performed with total RNA extracted from IC177 cells grown on carbazole. The primers were designed to generate PCR products encompassing the tandemly linked genes, as shown in Fig. 2. Whereas PCR without RT did not show any amplification products, RT-PCR produced products of the expected sizes (Fig. 2). These data showed that the *carAa*, *-C*, *-Ba*, *-Bb*, *-Ac*, and *-Ad* genes and the *carD*, *-F*, and *-E* genes are transcribed as respective operons.

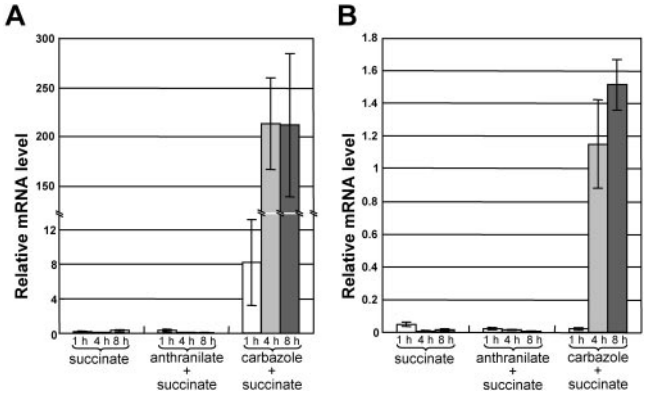

FIG. 3. Quantitative RT-PCR analysis of *carAa* (A) and *carD* (B) mRNAs. mRNA levels of *carAa* and *carD* in *N. aromaticivorans* IC177 were normalized to that of *rrn*. Times for incubation and exposure to the substrates in succinate-grown IC177 cells are shown.

To analyze the inducibility of the *car* operons, we performed quantitative RT-PCR, using two pairs of primers specific for *carAa* and *carD*. IC177 cells grown on succinate were exposed to succinate alone, anthranilate plus succinate, or carbazole plus succinate. Total RNA was extracted from each sample after 1, 4, or 8 h of incubation. Compared to the negative control samples containing no reverse transcriptase or template, very low levels of *carAa* and *carD* mRNAs were detected at all stages in cells incubated with succinate alone or anthranilate plus succinate (data not shown). The expression levels of both *carAa* and *carD* did not change upon exposure to anthranilate. These results show that anthranilate, an intermediate of the carbazole degradation pathway (Fig. 1), is not the inducer of the *car* operons of IC177, although anthranilate is an inducer of the CA10 *car* operon (55). *carAa* expression was inducible in cells exposed to carbazole (Fig. 3A), and the *carAa* mRNA level at 1 h in the presence of carbazole plus succinate was approximately 42-fold higher than that in the presence of anthranilate plus succinate or succinate alone (Fig. 3A). Further incubation with carbazole plus succinate led to a higher level of *carAa* expression (approximately 26-fold higher than that after 1 h of incubation). *carD* expression was also induced in cells incubated with carbazole plus succinate (Fig. 3B). However, the incubation time for induction of *carD* expression was 4 h, which differed from that for *carAa* (Fig. 3).

Expression of *carAa*, *carAc*, *carAd*, *carBa*, *carBb*, and *carC* genes in *E. coli*. The sequencing analysis and gene expression data indicated that the *carAa*, *-Ac*, and *-Ad* genes encode a carbazole dioxygenase responsible for the growth of IC177 on carbazole. To confirm the role of initial oxygenation of carbazole, the *carAa*, *-Ac*, and *-Ad* genes were cloned and expressed in *E. coli*. The *carAa*, *carAaAc*, *carAaAd*, *carAcAd*, and *carAaAcAd* genes were cloned into pBluescript II SK(−), and

the resultant plasmids were designated pB177301, pB177304, pB177305, pB177306, and pB177307, respectively. The ability of *E. coli* JM109 carrying each plasmid to transform carbazole to 2′-aminobiphenyl-2,3-diol after IPTG induction was analyzed. *E. coli* JM109(pB177307), expressing *carAaAcAd*, completely (>99%) transformed carbazole to 2′-aminobiphenyl-2,3-diol in 24 h. These data indicate that the gene products of *carAaAcAd* function as the angular dioxygenase for carbazole. The angular dioxygenase catalyzes the dihydroxylation of carbazole at an angular positioned carbon (C-9a) binding to the imino nitrogen and the adjacent C-1 carbon (Fig. 1). After 24 h of incubation, *E. coli* JM109(pB177304), expressing *carAaAc*, oxidized 2.3% of the carbazole, suggesting that the ferredoxin (CarAc) had the ability to accept electrons from unidentified *E. coli* reductases with a much lower efficiency than that from its own natural reductase (CarAd). *E. coli* JM109 carrying pB177301 (*carAa*), pB177305 (*carAaAd*), and pB177306 (*carAcAd*) did not transform carbazole at all. These data demonstrate that *carAc* and *carAd* encode a specific ferredoxin and ferredoxin reductase, respectively, which act together with the terminal oxygenase component to transform carbazole to 1,9a-dihydroxy-1-hydrocarbazole, which is considered to be spontaneously converted to 2′-aminobiphenyl-2,3-diol (Fig. 1).

The functionality of the *carBaBbC* gene products was also tested by measuring their enzymatic activity in *E. coli*. We constructed plasmids containing the *carAaAcAdBa*, *carAaAcAdBaBb*, and *carAaAcAdBaBbC* genes under control of the *lac* promoter and designated them pB177308, pB177309, and pB177310, respectively. A colony of *E. coli* harboring pB177309 grown in LB medium containing 1 mM IPTG showed production of a yellow compound after being sprayed with ethereal 2,3-dihydroxybiphenyl, which is an analog of 2′-aminobiphenyl-2,3-diol, although no production of the yellow compound was observed on *E. coli* harboring pB177308 prepared as a negative control (data not shown). This result indicates that the *carBaBb* gene products function as *meta*-cleavage enzymes in the catabolism of carbazole in IC177, as shown in Fig. 1.

To confirm the function of the *carC* gene product, we also analyzed its reaction in resting cells. The ability of *E. coli* JM109 expressing CarC in conjunction with CarAaAcAdBaBb to transform carbazole to anthranilate was analyzed. Although no production of anthranilate was detected in *E. coli* cells carrying pBluescriptII SK(−), anthranilate (approximately 2% of the remaining carbazole) was clearly detected in the cell suspension of *E. coli* expressing *carAaAcAdBaBbC* incubated with carbazole. Thus, it was confirmed that the *carBaBbC* gene products possess the expected functions in the conversion of carbazole to anthranilate, as shown in Fig. 1.

Substrate preference of CarAaAcAd. To analyze the substrate preference of the CARDO of IC177, *E. coli* carrying pB177307 (containing *carAaAcAd*) was tested for the ability to convert several aromatic compounds, including biphenyl, naphthalene, 9-fluorenone, fluorene, dibenzothiophene sulfone, dibenzo-*p*-dioxin, dibenzofuran, and carbazole. The products were identified by comparison to the retention times and MS patterns of GC-MS data from previous experiments (21, 38, 53). Among the seven aromatic compounds, naphthalene was the most efficiently transformed (Table 3). The lateral dioxygenation product, *cis*-1,2-dihydroxy-1,2-dihydronaphthalene, and its putative dehydrated derivative, 1-naphthol, were detected (Table 3). Significant transformation was also observed for dibenzo-*p*-dioxin, and only the angular dioxygenation product (2,2′,3-trihydroxydiphenyl ether) was detected. Weak transformation of biphenyl to *cis*-2,3-dihydroxy-2,3-dihydrobiphenyl (with 2-hydroxybiphenyl, a putative dehydrated derivative from *cis*-2,3-dihydroxy-2,3-dihydrobiphenyl), fluorene to 9-hydroxyfluorene and dihydrodiol (lateral dioxygenation product) (53), and dibenzofuran to 2,2′,3-trihydroxybiphenyl was also detected (Table 3). Other putative oxygenation products were not detected in this analysis.

TABLE 3. Biotransformation analysis using *E. coli* expressing carbazole 1,9a-dioxygenase from *N. aromaticivorans* IC177

Substrate	Detected compound[a]	Conversion ratio (%)[b]
Naphthalene	*cis*-1,2-Dihydroxy-1,2-dihydronaphthalene	47 (±4.8)
	1-Naphthol	53 (±4.8)
Carbazole	2′-Aminobiphenyl-2,3-diol	96 (±4.6)
Dibenzo-*p*-dioxin	2,2′,3-Trihydroxydiphenyl ether	69 (±2.5)
Dibenzofuran	2,2′,3-Trihydroxybiphenyl	8.8 (±0.75)
Biphenyl	*cis*-2,3-Dihydroxy-2,3-dihydroxybiphenyl	3.5 (±0.63)
	2-Hydroxybiphenyl	2.7 (±0.24)
	Biphenyl dihydrodiol	0.50 (±0.15)
Fluorene	9-Hydroxyfluorene	1.6 (±0.25)
	Dihydrodiol	1.9 (±0.51)
9-Fluorenone	ND[c]	
Dibenzothiophene sulfone	ND[c]	

[a] Products were identified by GC-MS analysis and compared to reported GC-MS data (21, 38, 53). These compounds also contained the products derived by nonenzymatic dehydration.

[b] Conversion ratio (%) = 100 × (peak area for the total ion current [TIC] of the product)/(peak area for substrate TIC + peak area for the TIC of all identified products). Values in parentheses represent standard deviations calculated from at least three assays.

[c] ND, no product was detected in this analysis.

DISCUSSION

We have studied the diversity of the carbazole catabolic genes and isolated several carbazole degraders and their *car* genes. To explain the evolutionary relationships of each carbazole catabolic gene, we analyzed the structures of the *car* genes and their flanking regions from several carbazole-degrading bacteria (18, 19, 40). The gene order of the *carC* and *carBaBb* genes in IC177 was inverted relative to that in well-characterized *car* gene clusters of the gram-negative bacteria *P. resinovorans* CA10, *Janthinobacterium* sp. strain J3, and *Sphingomonas* sp. strain KA1 (Fig. 4). In the *carAaCBaBbAcAd* and *carDFE* operons in IC177, all of the genes overlap each other by 1 or 4 bp (data not shown), while such complete overlap was not observed in *car* gene clusters from gram-negative bacteria. In addition, the *carAc* gene was separated from the *carAd* gene by an ORF of unknown function in CA10 and J3 (Fig. 4). As for the two *car* gene clusters of KA1, there was no gene corresponding to *carAd* and encoding NAD(P)H:ferredoxin oxidoreductase in the neighboring region of the *car* gene cluster (Fig. 4). Moreover, in CA10, *carD* was separated from the *carFE* genes by two unknown ORFs, and these genes were located downstream of the *carAaBaBbCAcAd* gene cluster,

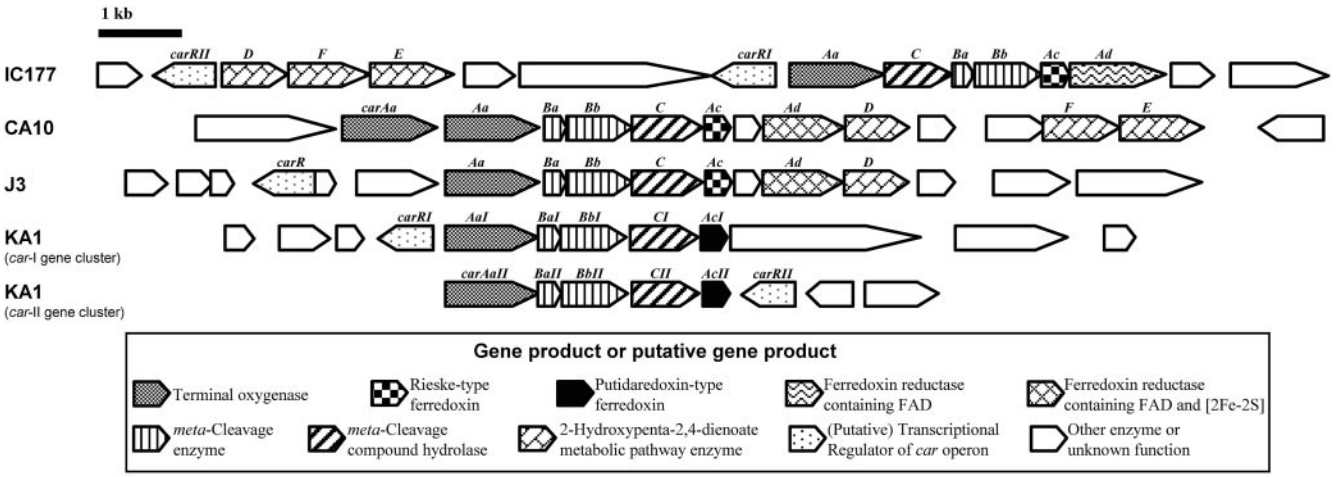

FIG. 4. Comparison of gene organization around the *car* gene clusters of *N. aromaticivorans* IC177, *P. resinovorans* CA10, *Janthinobacterium* sp. strain J3, and *Sphingomonas* sp. strain KA1. The pentagons indicate the sizes, locations, and directions of gene or ORF transcription.

implying that the *carFE* genes were recruited into the *car* gene cluster during the late phase of the evolutionary process (19). However, the *carDFE* genes were closely linked and located upstream of the *carAaCBaBbAcAd* gene cluster in IC177. These results suggest a unique evolutionary history of carbazole catabolic genes in IC177. Many genes involved in the degradation of aromatic compounds are organized into operons or functional units (57). The carbazole catabolic operons of IC177 are organized more orderly as functional units than those in gram-negative strains, such as CA10, J3, and KA1.

Various ROSs have been identified and extensively studied, mainly as the initial oxygenases of aromatic compounds (5, 11, 14, 17, 29, 58). The known CARDOs from *P. resinovorans* CA10, *Sphingomonas* sp. strain KA1, and *Sphingomonas* sp. strain GTIN11 are class III, IIA, and IIA enzymes, respectively (19, 24, 47). In addition, a phylogenetically less-related CARDO was isolated from *Sphingomonas* sp. strain CB3 (50). Although the *car* genes of CB3 are transcribed in carbazole-grown CB3 cells, the enzymatic activity of the CARDO was not directly detected (50). Thus, we excluded the CARDO of CB3 from our discussion on the electron transfer functions of CARDOs. The terminal oxygenase of IC177 was closely related to the CARDOs from CA10 and J3 (class III) and from KA1 (class IIA) (>45% identity) (see Fig. S1A in the supplemental material), and the ferredoxin of IC177 was a Rieske-type ferredoxin similar to that of CA10, even though they did not have phylogenetically very close relationships with each other (see Fig. S1B in the supplemental material). The amino acid sequence of the ferredoxin reductase component (CarAd) from IC177 showed high homology with the NAD(P)H:ferredoxin oxidoreductases from class IIB ROSs (see Fig. S1C in the supplemental material). It did not contain the consensus sequence of plant-type iron-sulfur proteins for the binding of a [2Fe-2S] cluster which is found in the ferredoxin reductase component of CA10. On the basis of these findings, the CARDO of IC177 belongs to class IIB. It is noteworthy that the terminal oxygenase components of the CARDOs from CA10/J3, KA1, and IC177 have substantial homology with each other (>45%) but that their electron transfer components are completely different. It would be interesting to learn how such similar terminal oxygenases can accept electrons from such diverse electron transfer components among the three CARDOs. Further biochemical and protein structural studies of these CARDOs will provide important information on the interactions of the electron transfer proteins and the enzyme evolutionary mechanisms.

The substrate preference of IC177 CARDO differed from those of CA10 and KA1. The CARDOs from CA10 and KA1 have high enzyme activities toward biphenyl and dibenzofuran (38, 53, 56), although these compounds were not good substrates for IC177 CARDO. Therefore, the CARDO of IC177 has a stronger preference for carbazole than those of CA10 and KA1. Recently, the crystal structure of a terminal oxygenase of CARDO from *Janthinobacterium* sp. strain J3 was determined (36). Some hydrophobic residues, such as Ile184, Ile186, Leu270, Val272, Phe275, Phe329, and Ile334, in CarAa of J3 were found to comprise substrate-binding pockets. In the terminal oxygenase of IC177, the residues corresponding to Ile186 and Ile334 of J3 are replaced by Met192 and Val338, respectively, although these residues are conserved in KA1. The difference in substrate specificity may result from the replacement of these amino acid residues. These residues for substrate binding are not conserved in either the naphthalene or biphenyl dioxygenase (6, 12); therefore, it will be important to determine which amino acid residues are involved in determining CARDO's substrate preference. In a previous study, we demonstrated that IC177 can grow on dibenzothiophene sulfone as the sole carbon source (18). There are several reports on dibenzothiophene sulfone- and 9-fluorenone-degrading bacteria suggesting that they convert these two compounds to angular dioxygenation products (4, 37). However, no plausible oxidation product was formed by IC177 CARDO with dibenzothiophene sulfone and 9-fluorenone. Thus, there may be a series of genes for the degradation of dibenzothiophene sulfone in another locus of the IC177 genome.

The (putative) regulatory proteins of the *car* gene clusters of IC177, CA10, J3, and KA1 are located differently in the neighboring regions of each *car* gene cluster (Fig. 4). Moreover, CarRI of IC177 showed similarity to transcriptional regulators

in the IclR family, although the transcriptional regulators of the *car* operons of CA10 and J3 are the AraC/Xyl family protein AntR (55) and the GntR family protein CarR (31), respectively. Therefore, the transcriptional regulatory systems of the *car* genes of IC177, CA10, and J3 are all different, although the carbazole catabolic genes are similar. Many related catabolic pathways do not carry the same regulatory system, which led to the hypothesis that regulatory systems and their target operons do not necessary coevolve but seem to become associated independently (7, 8, 54). The differences in the regulatory systems of carbazole catabolic genes in CA10, J3, and IC177 also support this hypothesis. It would be interesting to determine which conditions cause the regulators from each strain to activate their *car* operons and how the activities of the translated products differ from each other.

From the results of qRT-PCR, the *carAa* gene was induced by exposure to carbazole within 1 h, although it took 4 h to detect the transcription of *carD*, implying a difference between the inducers of the *carAaCBaBbAcAd* and *carDFE* operons. In the carbazole degradation pathway, the gene products of the *carAaCBaBbAcAd* operon are responsible for the upper pathway of carbazole degradation, while those of the *carDFE* operon are responsible for the lower pathway (*meta*-pathway) (Fig. 1). Thus, it is reasonable that the *carAaCBaBbAcAd* operon is more promptly transcribed than the *carDFE* operon after application of the substrate.

ACKNOWLEDGMENT

This work was supported by grants from the Program for Promotion of Basic Research Activities for Innovative Bioscience (PROBRAIN).

REFERENCES

1. **Arcos, J. C., and M. F. Argus.** 1968. Molecular geometry and carcinogenic activity of aromatic compounds. New perspectives. Adv. Cancer Res. **11:**305–471.
2. **Batie, C. J., D. P. Ballou, and C. C. Correll.** 1991. Phthalate dioxygenase reductase and related flavin-iron-sulfur containing electron transferases, p. 543–556. *In* F. Muller (ed.), Chemistry and biochemistry of flavoenzymes, vol. 3. CRC Press, Boca Raton, Fla.
3. **Benedik, M. J., P. R. Gibbs, R. R. Riddle, and R. C. Willson.** 1998. Microbial denitrogenation of fossil fuels. Trends Biotechnol. **16:**390–395.
4. **Bressler, D. C., and P. M. Fedorak.** 2000. Bacterial metabolism of fluorene, dibenzofuran, dibenzothiophene, and carbazole. Can. J. Microbiol. **46:**397–409.
5. **Butler, C. S., and J. R. Mason.** 1997. Structure-function analysis of the bacterial aromatic ring-hydroxylating dioxygenases. Adv. Microb. Physiol. **38:**47–84.
6. **Carredano, E., A. Karlsson, B. Kauppi, D. Choudhury, R. E. Parales, J. V. Parales, K. Lee, D. T. Gibson, H. Eklund, and S. Ramaswamy.** 2000. Substrate binding site of naphthalene 1,2-dioxygenase: functional implications of indole binding. J. Mol. Biol. **296:**701–712.
7. **Cases, I., and V. de Lorenzo.** 2001. The black cat/white cat principle of signal integration in bacterial promoters. EMBO J. **20:**1–11.
8. **Cases, I., and V. de Lorenzo.** 2005. Promoters in the environment: transcriptional regulation in its natural context. Nat. Rev. Microbiol. **3:**105–118.
9. **Cho, Y. G., J. H. Yoon, Y. H. Park, and S. T. Lee.** 1998. Simultaneous degradation of *p*-nitrophenol and phenol by a newly isolated *Nocardioides* sp. J. Gen. Appl. Microbiol. **44:**303–309.
10. **Colbert, C. L., M. M.-J. Couture, L. D. Eltis, and J. T. Bolin.** 2000. A cluster exposed: structure of the Rieske ferredoxin from biphenyl dioxygenase and redox properties of Rieske Fe-S proteins. Structure **8:**1267–1278.
11. **Ferraro, D. J., L. Gakhar, and S. Ramaswamy.** 2005. Rieske business: structure-function of Rieske non-heme oxygenases. Biochem. Biophys. Res. Commun. **338:**175–190.
12. **Furusawa, Y., V. Nagarajan, M. Tanokura, E. Masai, M. Fukuda, and T. Senda.** 2004. Crystal structure of the terminal oxygenase component of biphenyl dioxygenase derived from *Rhodococcus* sp. strain RHA1. J. Mol. Biol. **342:**1041–1052.
13. **Futamata, H., T. Uchida, N. Yoshida, Y. Yonemitsu, and A. Hiraishi.** 2004. Distribution of dibenzofuran-degrading bacteria in soils polluted with different levels of polychlorinated dioxins. Microbes Environ. **19:**172–177.
14. **Gibson, D. T., and R. E. Parales.** 2000. Aromatic hydrocarbon dioxygenases in environmental biotechnology. Curr. Opin. Biotechnol. **11:**236–243.
15. **Golovleva, L. A., R. N. Pertsova, L. I. Evtushenko, and B. P. Baskunov.** 1990. Degradation of 2,4,5-trichlorophenoxyacetic acid by a *Nocardioides simplex* culture. Biodegradation **1:**263–271.
16. **Habe, H., Y. Ashikawa, Y. Saiki, T. Yoshida, H. Nojiri, and T. Omori.** 2002. *Sphingomonas* sp. strain KA1, carrying a carbazole dioxygenase gene homologue, degrades chlorinated dibenzo-*p*-dioxins in soil. FEMS Microbiol. Lett. **211:**43–49.
17. **Harayama, S., and M. Kok.** 1992. Functional and evolutionary relationships among diverse oxygenases. Annu. Rev. Microbiol. **46:**565–601.
18. **Inoue, K., H. Habe, H. Yamane, T. Omori, and H. Nojiri.** 2005. Diversity of carbazole-degrading bacteria having the *car* gene cluster: isolation of a novel gram-positive carbazole-degrading bacterium. FEMS Microbiol. Lett. **245:**145–153.
19. **Inoue, K., J. Widada, S. Nakai, T. Endoh, M. Urata, Y. Ashikawa, M. Shintani, Y. Saiki, T. Yoshida, H. Habe, T. Omori, and H. Nojiri.** 2004. Divergent structures of carbazole degradative *car* operons isolated from gram-negative bacteria. Biosci. Biotechnol. Biochem. **70:**1467–1480.
20. **Iwabuchi, T., Y. Inomata-Yamauchi, A. Katsuta, and S. Harayama.** 1998. Isolation and characterization of marine *Nocardioides* capable of growing and degrading phenanthrene at 42°C. J. Mar. Biotechnol. **6:**86–90.
21. **Kasuga, K., H. Nojiri, H. Yamane, T. Kodama, and T. Omori.** 1997. Cloning and characterization of the genes involved in the degradation of dibenzofuran by *Terrabacter* sp. strain DBF63. J. Ferment. Bioeng. **84:**387–399.
22. **Kikuchi, Y., Y. Nagata, M. Hinata, K. Kimbara, M. Fukuda, K. Yano, and M. Takagi.** 1994. Identification of the *bphA4* gene encoding ferredoxin reductase involved in biphenyl and polychlorinated biphenyl degradation in *Pseudomonas* sp. strain KKS102. J. Bacteriol. **176:**1689–1694.
23. **Kikuchi, Y., Y. Yasukochi, Y. Nagata, M. Fukuda, and M. Takagi.** 1994. Nucleotide sequence and functional analysis of the *meta*-cleavage pathway involved in biphenyl and polychlorinated biphenyl degradation in *Pseudomonas* sp. strain KKS102. J. Bacteriol. **176:**4269–4276.
24. **Kilbane, J. J., II, A. Daram, J. Abbasian, and K. J. Kayser.** 2002. Isolation and characterization of *Sphingomonas* sp. GTIN11 capable of carbazole metabolism in petroleum. Biochem. Biophys. Res. Commun. **297:**242–248.
25. **Kubota, M., K. Kawahara, K. Sekiya, T. Uchida, Y. Hattori, H. Futamata, and A. Hiraishi.** 2005. *Nocardioides aromaticivorans* sp. nov., a dibenzofuran-degrading bacterium isolated from dioxin-polluted environments. Syst. Appl. Microbiol. **28:**165–174.
26. **Lau, P. C. K., H. Bergeron, D. Labbé, Y. Wang, R. Brousseau, and D. T. Gibson.** 1994. Sequence and expression of the *todGIH* genes involved in the last three steps of toluene degradation by *Pseudomonas putida* F1. Gene **146:**7–13.
27. **Manjasetty, B. A., J. Powlowski, and A. Vrielink.** 2003. Crystal structure of a bifunctional aldolase-dehydrogenase: sequestering a reactive and volatile intermediate. Proc. Natl. Acad. Sci. USA **100:**6992–6997.
28. **Masai, E., K. Sugiyama, N. Iwashita, S. Shimizu, J. E. Hauschild, T. Hatta, K. Kimbara, K. Yano, and M. Fukuda.** 1997. The *bphDEF meta*-cleavage pathway genes involved in biphenyl/polychlorinated biphenyl degradation are located on a linear plasmid and separated from the initial *bphACB* genes in *Rhodococcus* sp. strain RHA1. Gene **187:**141–149.
29. **Mason, J. R., and R. Cammack.** 1992. The electron-transport proteins of hydroxylating bacterial dioxygenases. Annu. Rev. Microbiol. **46:**277–305.
30. **McCarthy, A. J., and S. T. Williams.** 1992. Actinomycetes as agents of biodegradation in the environment—a review. Gene **115:**189–192.
31. **Miyakoshi, M., M. Urata, H. Habe, T. Omori, H. Yamane, and H. Nojiri.** 2006. Differentiation of carbazole catabolic operons by replacement of the regulated promoter via transposition of an insertion sequence. J. Biol. Chem. **281:**8450–8457.
32. **Mueller, J. G., P. J. Chapman, and P. H. Pritchard.** 1989. Creosote-contaminated sites: their potential for bioremediation. Environ. Sci. Technol. **23:**1197–1201.
33. **Mushrush, G. W., E. J. Beal, D. R. Hardy, and J. M. Hughes.** 1999. Nitrogen compound distribution in middle distillate fuels derived from petroleum, oil shale, and tar sand sources. Fuel Process. Technol. **61:**197–210.
34. **Nam, J.-W., H. Noguchi, Z. Fujimoto, H. Mizuno, Y. Ashikawa, M. Abo, S. Fushinobu, N. Kobayashi, T. Wakagi, K. Iwata, T. Yoshida, H. Habe, H. Yamane, T. Omori, and H. Nojiri.** 2005. Crystal structure of the ferredoxin component of carbazole 1,9a-dioxygenase of *Pseudomonas resinovorans* strain CA10, a novel Rieske non-heme iron oxygenase system. Proteins **58:**779–789.
35. **Nam, J.-W., H. Nojiri, H. Noguchi, H. Uchimura, T. Yoshida, H. Habe, H. Yamane, and T. Omori.** 2002. Purification and characterization of carbazole 1,9a-dioxygenase, a three-component dioxygenase system of *Pseudomonas resinovorans* strain CA10. Appl. Environ. Microbiol. **68:**5882–5890.
36. **Nojiri, H., Y. Ashikawa, H. Noguchi, J.-W. Nam, M. Urata, Z. Fujimoto, H. Uchimura, T. Terada, S. Nakamura, K. Shimizu, T. Yoshida, H. Habe, and T. Omori.** 2005. Structure of the terminal oxygenase component of angular dioxygenase, carbazole 1,9a-dioxygenase. J. Mol. Biol. **351:**355–370.
37. **Nojiri, H., H. Habe, and T. Omori.** 2001. Bacterial degradation of aromatic compounds via angular dioxygenation. J. Gen. Appl. Microbiol. **47:**279–305.

38. **Nojiri, H., J.-W. Nam, M. Kosaka, K. Morii, T. Takemura, K. Furihata, H. Yamane, and T. Omori.** 1999. Diverse oxygenations catalyzed by carbazole 1,9a-dioxygenase from *Pseudomonas* sp. strain CA10. J. Bacteriol. **181:**3105–3113.
39. **Nojiri, H., and T. Omori.** 2002. Molecular bases of aerobic bacterial degradation of dioxins: involvement of angular dioxygenation. Biosci. Biotechnol. Biochem. **66:**2001–2016.
40. **Nojiri, H., H. Sekiguchi, K. Maeda, M. Urata, S. Nakai, T. Yoshida, H. Habe, and T. Omori.** 2001. Genetic characterization and evolutionary implications of a *car* gene cluster in the carbazole degrader *Pseudomonas* sp. strain CA10. J. Bacteriol. **183:**3663–3679.
41. **Ouchiyama, N., Y. Zhang, T. Omori, and T. Kodama.** 1993. Biodegradation of carbazole by *Pseudomonas* spp. CA06 and CA10. Biosci. Biotechnol. Biochem. **57:**455–460.
42. **Page, R. D. M.** 1996. Treeview: an application to display phylogenetic trees on personal computers. Comput. Appl. Biosci. **12:**357–358.
43. **Parales, R. E.** 2003. The role of active-site residues in naphthalene dioxygenase. J. Ind. Microbiol. Biotechnol. **30:**271–278.
44. **Pinyakong, O., H. Habe, T. Yoshida, H. Nojiri, and T. Omori.** 2003. Identification of three novel salicylate 1-hydroxylases involved in the phenanthrene degradation of *Sphingomonas* sp. strain P2. Biochem. Biophys. Res. Commun. **301:**350–357.
45. **Rajan, J., K. Valli, R. E. Perkins, F. S. Sariaslani, S. M. Barns, A. L. Reysenbach, S. Rehm, M. Ehringer, and N. R. Pace.** 1996. Mineralization of 2,4,6-trinitrophenol (picric acid): characterization and phylogenetic identification of microbial strains. J. Ind. Microbiol. **16:**319–324.
46. **Sambrook, J., and D. W. Russell.** 2001. Molecular cloning: a laboratory manual, 3rd ed. Cold Spring Harbor Laboratory Press, Cold Spring Harbor, N.Y.
47. **Sato, S., J.-W. Nam, K. Kasuga, H. Nojiri, H. Yamane, and T. Omori.** 1997. Identification and characterization of genes encoding carbazole 1,9a-dioxygenase in *Pseudomonas* sp. strain CA10. J. Bacteriol. **179:**4850–4858.
48. **Sato, S., N. Ouchiyama, T. Kimura, H. Nojiri, H. Yamane, and T. Omori.** 1997. Cloning of genes involved in carbazole degradation of *Pseudomonas* sp. strain CA10: nucleotide sequences of genes and characterization of *meta*-cleavage enzymes and hydrolase. J. Bacteriol. **179:**4841–4849.
49. **Senda, T., T. Yamada, N. Sakurai, M. Kubota, T. Nishizaki, E. Masai, M. Fukuda, and Y. Mitsui.** 2000. Crystal structure of NADH-dependent ferredoxin reductase component in biphenyl dioxygenase. J. Mol. Biol. **304:**397–410.
50. **Shepherd, J. M., and G. Lloyd-Jones.** 1998. Novel carbazole degradation genes of *Sphingomonas* CB3: sequence analysis, transcription, and molecular ecology. Biochem. Biophys. Res. Commun. **247:**129–135.
51. **Shine, J., and L. Dalgano.** 1975. Determination of cistron specificity in bacteria ribosomes. Nature **254:**34–38.
52. **Shingler, V., J. Powlowski, and U. Marklund.** 1992. Nucleotide sequence and functional analysis of the complete phenol/3,4-dimethylphenol catabolic pathway of *Pseudomonas* sp. strain CF600. J. Bacteriol. **174:**711–724.
53. **Takagi, T., H. Nojiri, T. Yoshida, H. Habe, and T. Omori.** 2002. Detailed comparison between the substrate specificities of two angular dioxygenases, dibenzofuran 4,4a-dioxygenase from *Terrabacter* sp. and carbazole 1,9a-dioxygenase from *Pseudomonas resinovorans*. Biotechnol. Lett. **24:**2099–2106.
54. **Tropel, D., and J. R. van der Meer.** 2004. Bacterial transcriptional regulators for degradation pathways of aromatic compounds. Microbiol. Mol. Biol. Rev. **63:**474–500.
55. **Urata, M., M. Miyakoshi, S. Kai, K. Maeda, H. Habe, T. Omori, H. Yamane, and H. Nojiri.** 2004. Transcriptional regulation of the *ant* operon, encoding two-component anthranilate 1,2-dioxygenase, on the carbazole-degradative plasmid pCAR1 of *Pseudomonas resinovorans* strain CA10. J. Bacteriol. **186:**6815–6823.
56. **Urata, M., H. Uchimura, H. Noguchi, T. Sakaguchi, T. Takemura, K. Eto, H. Habe, T. Omori, H. Yamane, and H. Nojiri.** 2006. Plasmid pCAR3 contains multiple gene sets involved in the conversion of carbazole to anthranilate. Appl. Environ. Microbiol., **72:**3206–3216.
57. **van der Meer, J. R., W. M. de Vos, S. Harayama, and A. J. B. Zehnder.** 1992. Molecular mechanisms of genetic adaptation to xenobiotic compounds. Microbiol. Rev. **56:**677–694.
58. **Wackett, L. P.** 2002. Mechanism and applications of Rieske non-heme iron dioxygenases. Enzyme Microb. Technol. **31:**577–587.